

# Optical Properties of Saharan Dust Aerosols, Sea Spray and Cloud Droplets from AMISOC-ARN 2012 airborne campaign

Javier Andrey<sup>1</sup>, Arturo Quirantes<sup>2</sup>, Neves Soane-Vieira<sup>3</sup>, Francisco José Olmo<sup>4</sup>,  
Lucas Alados-Arboledas<sup>5</sup>, Benito de la Morena<sup>6</sup>, Manuel Gil-Ojeda<sup>7</sup>

**Abstract** – In the frame of AMISOC-ARN project an airborne campaign was held at "El Arenosillo" sounding station in the south-west of the Iberian Peninsula. Three vertical profiles were developed by the INTA C212 atmospheric research aircraft characterizing aerosol size distribution and scattering properties among other parameters. Scattering cross sections measured by a CAS-DPOL optical particle counter have been used as input data for a new refractive index retrieval algorithm. Preliminary results from this algorithm show a good agreement with the different kind of aerosols sampled during the campaign. The uncertainties of the algorithm are lower for particles above 5-8  $\mu\text{m}$ , finding its maximum magnitude for particles in the range from 1 to 3  $\mu\text{m}$ .

**Keywords** – Airborne measurements, Refractive index, Size distribution, Tropospheric aerosols

## 1 INTRODUCTION

The largest uncertainty in estimating the Earth radiative balance is caused by aerosols [1]. Aerosols affect the solar radiation by scattering and absorption processes. The impact of each aerosol type on radiation depends in factors such as refractive index or particle shape.

In-situ characterizations of tropospheric aerosols provide valuable information about the state of these particles in the free troposphere. These characterizations require the use of airborne instrumentation on-board balloons or airplanes. The Spanish National Aerospace Technique Institute (INTA) owns an atmospheric research aircraft instrumented with different optical particle counters (OPC) devoted to the measurement of cloud and aerosol size distribution (SD). This kind of instruments is based on analyzing the scattered radiation at given directions and sizing the particles by using Mie theory.

In order to get the correct aerosol size with an OPC, a value for the particle refractive index must be assumed to carry out the corresponding Mie computations. The detection of the light scattered by one particle at different directions simultaneously allows to retrieve the aerosol refractive index of this particle. This procedure prevents making assumptions about this index, in order to get the correct size of the aerosol.

During late May and June of 2012, INTA carried out an airborne campaign in the frame of AMISOC (Atmospheric Minor Species relevant to the Ozone Chemistry at both sides of the subtropical jet) at "El arenosillo" sounding station (ARN) in the south of the Iberian Peninsula (IP). Several measurements of different gases and aerosols were carried out both on-board INTA aircraft and ground level, being this work focused in the CAS-DPOL (Cloud Aerosol Spectrometer with Depolarization Option) instrument, mounted on the aircraft. The latter provides measurements of scattered radiation in forward and backward directions for single particles. This combination of measurements allows to retrieve the real part of aerosol refractive index. Particle asphericity can also be derived by using an empirical approach based on three signals registered by the probe: forward, backward and polarized backward.

In this work, measurements from AMISOC-ARN campaign measurements are shown. These data are used to validate an algorithm devoted to retrieve the refractive index of aerosol particles sampled CAS-DPOL instrument.

<sup>1</sup>J. Andrey is with the Spanish National Aerospace Technique Institute (INTA), email: javier.andrey@gmail.com

<sup>2</sup>A. Quirantes is with the Andalusian Center for Environmental Research (CEAMA) and the Department of Applied Physics of Granada University (UGR), email: aquiran@ugr.es

<sup>3</sup>N. Soane-Vieira is with the Spanish National Aerospace Technique Institute (INTA), email: nevessoane@gmail.com

<sup>4</sup>F.J. Olmo is with the Andalusian Center for Environmental Research (CEAMA) and the Department of Applied Physics of Granada University (UGR), email: fjolmo@ugr.es

<sup>5</sup>L. Alados-Arboledas is with the Andalusian Center for Environmental Research (CEAMA) and the Department of Applied Physics of Granada University (UGR), email: alados@ugr.es

<sup>6</sup>B. de la Morena is with the Spanish National Aerospace Technique Institute (INTA), email: morenab@inta.es

<sup>7</sup>M. Gil-Ojeda is with the Spanish National Aerospace Technique Institute (INTA), email: gilm@inta.es

## 2 AMISOC-ARN 2012 CAMPAIGN

AMISOC is a research project funded by the Spanish R&D program devoted to improve the knowledge of minor constituents playing a role in ozone chemistry [2]. AMISOC-ARN campaign was conceived as a multi-instrumented campaign in order to study the behavior of minor trace gases under heavy aerosol loading. This situation is frequent in spring- and summertime when Saharan dust intrusions arrive to the SW-IP [3, 4].

ARN is a multi-instrumented platform for studying several topics on atmospheric sciences located in the coast of Huelva (N37.1 W6.7) near the Doñana national park. The main aerosol types at this sampling site are coastal marine, continental and desert dust. The main atmospheric circulations are the regional (sea-land breeze phenomenon) and synoptic-scale patterns. This observatory is equipped with different instrumentation for monitoring different parameters, such as aerosol (by in-situ and remote sensing techniques), gaseous pollutant concentration ( $O_3$ ,  $NO_2$  and  $NO_x$ ) and meteorological parameters.

### 2.1 Instrumentation

INTA C212-200 Aircraft is twin turboprop-powered medium transport designed and built by EADS-CASA as civil and military transport. This aircraft has a maximum payload of 2.800 kg. The ceiling service is 26.000 ft / 7.925 m. The cabin is not pressurized so oxygen is required when 10.000 ft / 3.000 m.a.s.l. of altitude is exceeded. It has been instrumented to carry out atmospheric studies keeping instrumentation both inside and outside the cabin. Two hard points are located under each wing to hold sondes from Droplet Measurements Technologies (DMT). Inlets for cabin instruments are located in the emergency trap aircraft behind the cockpit.

The CAS-DPOL instrument is part of the DMT multi-instrument *Cloud, Aerosol and Precipitation Sonde* (CAPS) which is compound by five instruments in total registering aerosol/cloud SD, liquid water content, cloud droplet 2D images, GPS position, pressure, temperature and relative humidity (RH). The CAS-DPOL installed on-board the C212 characterizes the aerosol SD through 30 channels in the range 0.5 to 50  $\mu\text{m}$  [5]. The forward detector collects the light scattered by the particles in the range of angle between  $4^\circ$  to  $12^\circ$  (fig. 1). This information is used by the probe to size the particles. Two additional detectors collect scattered light in backward direction ( $168^\circ$  to  $176^\circ$ ), being a linear polarizer in front of the second backward detector. Acquisition time and records from this three detectors are registered in a 'Particle By Particle' (PBP) file.

Temperature and relative humidity measurements from the CAPS instrument have been also used.

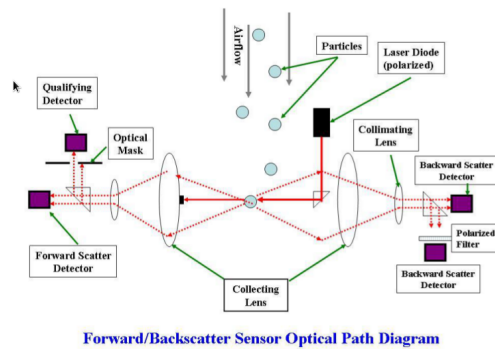


Figure 1: CAS-DPOL scheme taken from the instrument manual [5]

### 2.2 Flight Descriptions

AMISOC-ARN campaign took place from 21 May to 13 June being developed three flights in this period. The first and second flights took place on 31 May and 1 June, when a Saharan Air Layer (SAL) arrived to ARN. The third flight of the campaign was performed on 13 June, under no-SAL conditions, the last campaign available date.

The flight tracks described by the aircraft consisted in an ascent over ARN following spirals and a descent in steps to improve the quality of certain measurements at previously determined altitudes. The ceiling of the SAL flights was above 22.000 ft for the SAL flights, and 13.000 ft was the ceiling reached in the no-SAL flight.

## 3 METHODOLOGY

The refractive index algorithm has been run over the PBP files from the campaign taking around one hour and a half to analyze the approximated four millions particles registered. Ten different possible real components of the refractive index have been considered in this analysis.

### 3.1 Analysis of Acquired Vertical Profiles

Temperature, RH and CAS-DPOL aerosol SD measurements collected by the CAPS instruments over ARN have been averaged within 100 m layers. Temperature and RH profiles have been used to determine the boundary layer (BL) and detect the presence of cloud droplets. SD vertical profiles has also been plotted with the same purposes.

### 3.2 Calibration Curves from CAS-DPOL Detectors

The algorithms used to retrieve refractive indexes in an experiment require the knowledge of a-priori calibration curves. When a particle reaches the laser

beam of the probe it is illuminated scattering radiation, and the particle cross section (XS) is converted into an electrical signal expressed in terms of counts by each probe photo-detectors. The calibration curves of CAS-DPOL instrument relate the XS with the counts registered in the PBP file. The following steps are followed to determine them in the laboratory:

1. Particles of known size and refractive index are sampled by the instrument (Polystyrene Latex Spheres, PSL, and Glass Beads, GB).
2. The XS of these particles are determined by calculating the phase function of the particle, and integrating it in the angle range for each detector ( $4^{\circ}$ - $12^{\circ}$  for forward detector,  $XS_{fwd}$ , and  $168^{\circ}$ - $176^{\circ}$  for backward detector,  $XS_{bck}$  and  $XS_{dpol}$ ). [6] codes have been used for this purpose.
3. Particle count data stored in the PBP file are plotted using histograms for each detector. Three histograms from the PBP file are obtained.
4. The histogram class with maximum concentration is associated to the theoretically calculated XS.

### 3.3 Refractive Index Algorithm

The refractive index is derived using a look-up table that has the theoretical values for the forward and backward scattering cross sections as a function of refractive index. Fig. 2 shows various pairs of  $XS_{fwd}$  and  $XS_{bck}$  for three different refractive index. For large enough particles, the relationship of forward to backward XS remains fairly constant.

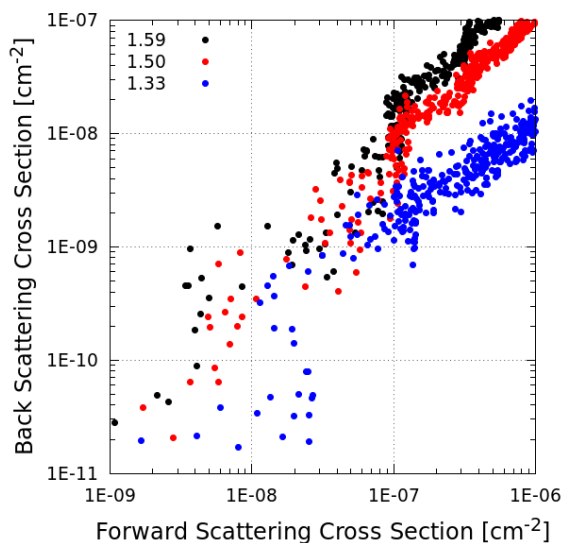


Figure 2: Forward and Backward scattering cross sections as a function of three different refractive indexes

The first step to derive the refractive index is to convert the counts information included in the PBP file into the corresponding  $XS_{fwd}$  and  $XS_{bck}$  through the calibration curves. After obtaining the particle XS a threshold around them is set up as an exact match will not be necessarily found when searching for occurrences in the lookup table. When a pair of forward and backward scattering cross sections is found that match those measured within the specified error for acceptance, this will indicate the refractive index for that particle.

In some cases, there may not be a unique answer, i.e., according to fig. 2 there are overlapping regions in the plot where particle with different refractive indexes correspond to similar pairs of XS. If the particle population is assumed to be composed of approximately the same composition, then for an ensemble of particles of many sizes, those sizes that have a unique forward to backward relationship will help decide the correct refractive index for those particles whose size is associated with more than one forward to backward scattering pair [5].

Note that in this work particles are assumed to be spherical as [6] does not consider aspherical particles. A posterior revision of the lookup table used in this work will include the code from [7] considering a 50% mix of oblate and prolate spheroids. In addition, the lookup tables used in this do not take into account any light absorption by the particles, i.e. the complex refractive indexes only include the real component. Tables can also be calculated to include imaginary components but this increases the complexity of the analysis as well as the resulting uncertainty.

## 4 RESULTS

A low pressure system located in the Sahara projected Saharan dust aerosols to the Atlantic being transported towards the IP. On the contrary to other SAL airborne campaigns developed by INTA [8, 9], a presence of clouds in the upper levels of the Saharan dust intrusion was observed (fig. 3).

As well as the previous flights, a depression system was located over the Sahara dessert, but the high pressure system located over the Azores archipelago prevent Saharan dust particles from the IP (fig. 4).

### 4.1 Vertical Profiles of Aerosols and Clouds in AMISOC-ARN Campaign

Vertical profiles of Temperature, RH and SD taken during the first flight are shown in fig. 5. The mixed Saharan dust-cloud layers observed by the crew during the SAL flights was located between 4 and 7 km above sea level (asl), where the RH increases up to 80%. The increase in larges particles concentration, above 5-8  $\mu\text{m}$ , is precisely associated to the RH incre-

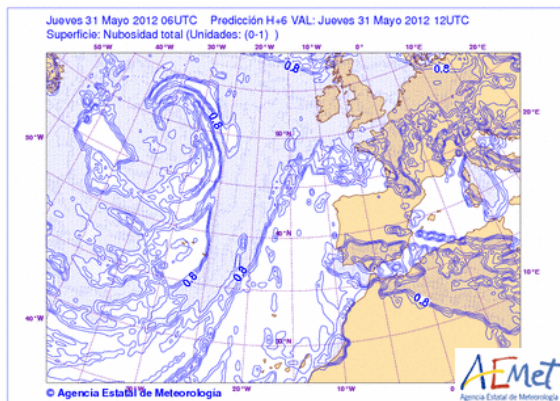


Figure 3: Cloudiness map from May 31, 2012. Data from the Spanish Meteorological Agency (AEMET)

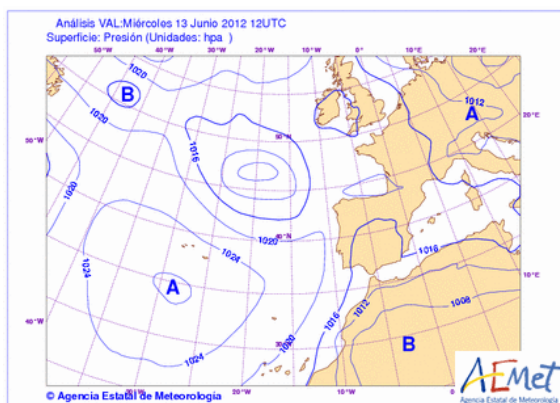


Figure 4: Pressure map from 13 June 2012. Data from the Spanish Meteorological Agency (AEMET)

ment, being these particles cloud droplets. No clear BL is observed both at RH or temperature profiles. The structure of vertical profiles taken during the first and second campaign flights are similar (fig. not shown). Two different groups of particles have been considered for the refractive index analysis: wet layer, between 4 and 7 km asl, and dry layer, from near sea surface up to 4 km asl considered as a pure Saharan dust aerosols layer.

A well-defined BL is observed around 2.1 km asl in the profile taken on June 13 (fig. 6). The particle concentrations observed in the SD profile are reduced precisely above this height. As the vertical profile was carried out over the sea with non-SAL conditions it has been assumed that aerosol particles observed are sea spray aerosols. BL and free troposphere (FT) layers have been configured to carry out the refractive index analysis.

#### 4.2 Refractive Index Analysis

Particles belonging to each of the four layers detailed in the previous section have been used as input data for the refractive index retrieval algorithm. This re-

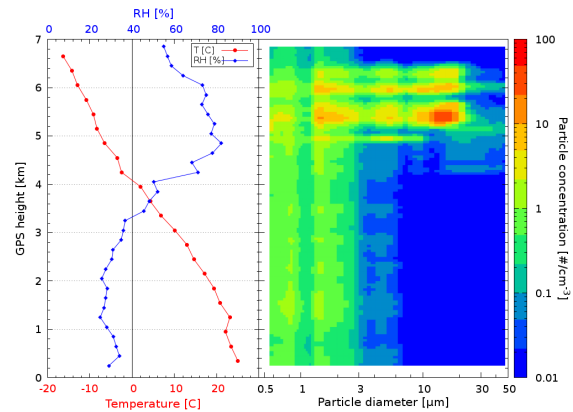


Figure 5: Vertical profiles of Temperature, RH and SD from the first AMISOC-ARN flight (31-May-2012).

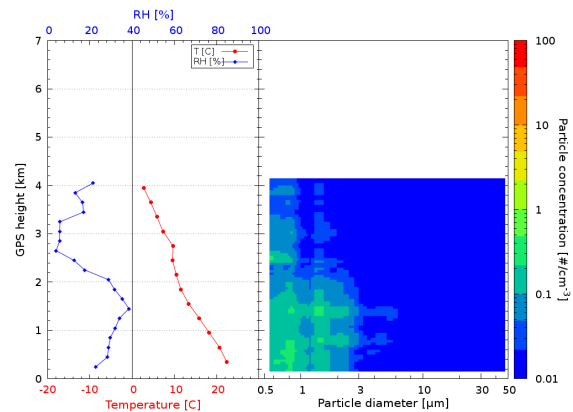


Figure 6: Vertical profiles of Temperature, RH and SD from the third AMISOC-ARN flight (13-June-2013).

sults have been classified into 10 classes according to ten possible real refractive indexes: 1.30, 1.33, 1.36, 1.39, 1.42, 1.46, 1.50, 1.53, 1.56 and 1.59. The frequency obtained for each class has been divided by the corresponding total number of particles analyzed in each layer with the aim to compare the results easily.

Fig. 7 shows the results obtained for the first campaign flight. The frequency of cloud droplets having a refractive index of 1.33 is higher in the wet layer than in the dry one as it was expected according to the RH profiles shown in fig. 5. A well formed peak is also found for particles with a refractive index value of 1.53. These particles correspond with Saharan dust aerosols which refractive index values reported by previous works is in the range from 1.53 to 1.56 [10, 11, 12].

Fig. 8 presents the results of the algorithm applied to the third flight data. The histogram corresponding to the BL shows two peaks, centered on the 1.33, and 1.53 classes. The first class should correspond with water droplets lifted from the sea, whereas the 1.53 class is associated with sea spray aerosols, which have a real refractive index of 1.50.

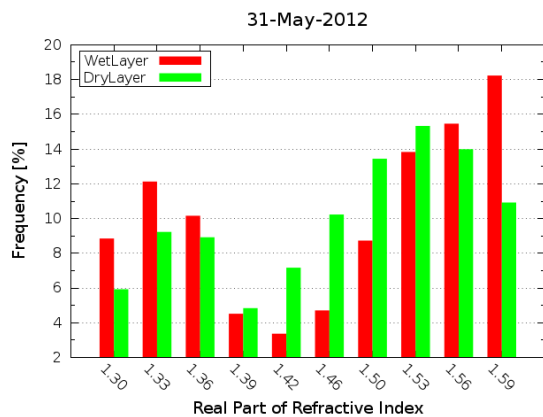


Figure 7: Refractive index algorithm results from the first flight on May 31. Frequencies are expressed in percent values.

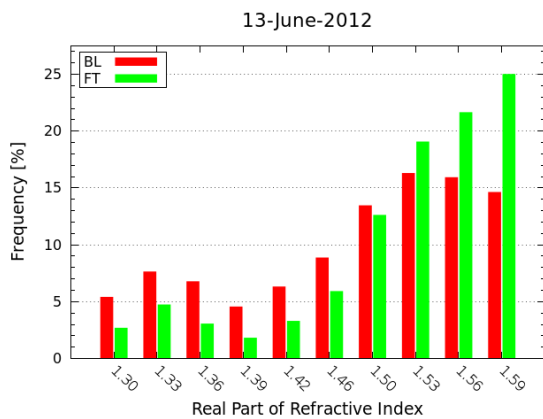


Figure 8: Refractive index algorithm results from the third campaign flight on June 13. Frequencies are expressed in percent values.

The high concentration of particles with a refractive index of 1.59 observed in the first flight wet layer and third flight FT layer apparently seems to be an artifact of the algorithm, as it tend to assign to sampled particles the same refractive index value than the one of the particles used during the calibration.

Although preliminary results show a good agreement with the expected results during AMISOC-ARN campaign, an error analysis must be performed. According to the lookup tables, the retrieval error for large particle (above 5-8  $\mu\text{m}$ ) is lower than for medium size particles (around 2.3  $\mu\text{m}$ ). A deeper analysis of retrieved refractive index values as a function of particle size is required to asses the algorithm uncertainties. This study is planned to be done before RICTA (*Reunión Ibérica de Ciencia y Tecnología de Aerosoles*) meeting on July 2013.

## 5 CONCLUSIONS

Data from AMISOC-ARN campaign were used to obtain preliminary results of a refractive index retrieval algorithm. This algorithm is based in the measurements of the CAS-DPOL OPC mounted on-board the INTA C212 atmospheric research aircraft. Three different kind of aerosols were sampled during AMISOC-ARN campaign.

Preliminary results show a good agreement with previously reported refractive indexes of Saharan Dust, sea spray and cloud droplets. Algorithm uncertainties will be presented in the RICTA 2013 meeting, at Evora on July 2013.

## ACKNOWLEDGEMENTS

The authors are grateful to INTA Aerial Platforms, belonging to the Spanish ICTS program, and the Spanish Air Force for their efforts maintaining and operating the aircraft. This work was supported by the Spanish Ministry for Economy and Competitiveness (MINECO) under grant CGL2011-24891 (AMISOC project). The Spanish Meteorological Agency (AEMET) is also thanked for their support during the airborne campaign. This work was supported by the Andalusia Regional Government through projects P08-RNM-3568 and P10-RNM-6299, by the Spanish Ministry of Science and Technology through projects CGL2010-18782, CSD2007-00067 and CGL2011-13580-E/CLI; and by EU through ACTRIS project (EU INFRA-2010-1.1.16-262254). The authors thankfully acknowledge the computer resources, technical expertise and assistance provided by the Barcelona Supercomputing Center. ALFA database computation was partly supported by RES (Spanish Supercomputation Network) computing resources (projects AECT-2009-1-0012, AECT-2011-3-0016).

## REFERENCES

- [1] IPCC, *Climate Change 2007: The Physical Science Basis. Contribution of Working Group I to the Fourth Assessment Report of the Intergovernmental Panel on Climate Change*. Cambridge University Press, Cambridge, United Kingdom and New York, NY, USA, 2007.
- [2] O. Puentedura, M. Gil, J. Adame, J. Andrey, C. Córdoba-Jabonero, L. Gómez, T. Hay, M. Navarro, C. Prados-Román, A. Saiz-López, M. Sorribas, D. Toledo, and B. de la Morena, "AMISOC 2012: Multi-instrumented campaign for gases-aerosols interaction assessment," in *European Aerosol Conference*, 2012.
- [3] C. Toledano, V. Cachorro, A. Berjon, A. De Frutos, M. Sorribas, B. De la Morena, and P. Goloub, "Aerosol optical depth and ångström exponent climatology at el arenosillo aeronet site (huelva, spain)," *Quarterly Journal of the Royal Meteorological Society*, vol. 133, no. 624, pp. 795–807, 2007.

- [4] C. Córdoba-Jabonero, M. Sorribas, J. Guerrero-Rascado, J. Adame, Y. Hernández, H. Lyamani, V. Cachorro, M. Gil, L. Alados-Arboledas, E. Cuevas, *et al.*, “Synergetic monitoring of saharan dust plumes and potential impact on surface: a case study of dust transport from canary islands to iberian peninsula,” *Atmospheric Chemistry and Physics Discussions*, vol. 10, pp. C11227–30, 2010.
- [5] Droplet Measurement Techniques (DMT), *The Cloud Aerosol Spectrometer – Depolarization Option (CAS-DPOL)*.
- [6] W. J. Wiscombe, “Improved mie scattering algorithms,” *Applied optics*, vol. 19, no. 9, pp. 1505–1509, 1980.
- [7] M. I. Mischenko, L. D. Travis, and A. A. Lacis, *Scattering, absorption, and emission of light by small particles*. Cambridge university press, 2002.
- [8] J. Andrey, M. Gil, and O. Serrano, “Size distribution vertical profiles of saharan dust over the eastern atlantic during the 2005-2006 summer outbreaks,” in *European Aerosol Conference*, (Salzburg, Austria), September 9-14 2007.
- [9] J. Andrey, M. Sorribas, J. Adame, M. Navarro-Comas, M. Gil, and B. de la Morena, “Vertical and ground base aerosols and gases characterization at ‘El Arenosillo’ station during July 2009,” in *VI Reunión Española de Ciencia y Tecnología de Aerosoles (RECTA 2011)*, 2011.
- [10] O. Dubovik, A. Smirnov, B. Holben, M. King, Y. Kaufman, T. Eck, and I. Slutsker, “Accuracy assessments of aerosol optical properties retrieved from Aerosol Robotic Network (AERONET) Sun and sky radiance measurements,” *JOURNAL OF GEOPHYSICAL RESEARCH-ATMOSPHERES*, vol. 105, pp. 9791–9806, APR 27 2000.
- [11] J. Haywood, P. Francis, S. Osborne, M. Glew, N. Loeb, E. Highwood, D. Tanré, G. Myhre, P. Formenti, and E. Hirst, “Radiative properties and direct radiative effect of saharan dust measured by the c-130 aircraft during shade: 1. solar spectrum,” *Journal of Geophysical Research: Atmospheres (1984–2012)*, vol. 108, no. D18, 2003.
- [12] A. Petzold, K. Rasp, B. Weinzierl, M. Esselborn, T. Hamburger, A. Dörnbrack, K. Kandler, L. Schütz, P. Knippertz, M. Fiebig, *et al.*, “Saharan dust absorption and refractive index from aircraft-based observations during samum 2006,” *Tellus B*, vol. 61, no. 1, pp. 118–130, 2009.
- [13] A. Quirantes, F. J. Olmo, H. Lyamani, and A. Valenzuela, “Investigation of fine and coarse aerosol contributions to the total aerosol light scattering: Shape effects and concentration profiling by raman lidar measurements,” *Journal of Quantitative Spectroscopy and Radiative Transfer*, 2012.